Order-restricted Bayesian Inference and Optimal Designs for the Simple Step-stress Accelerated Life Tests under Progressive Type-I Censoring based on Three-parameter Gamma Prior

Crystal Wiedner* David Han†

Abstract

In this work, we investigate the order-restricted Bayesian estimation and design optimization for a progressively Type-I censored simple step-stress accelerated life tests with exponential lifetimes under both continuous and interval inspections. Based on the three-parameter gamma distribution as a conditional prior, we ensure that the failure rates increase as the stress level increases. In addition, its conjugate-like structure enables us to derive the exact joint posterior distribution of the parameters without a need to perform an expensive MCMC sampling. Upon these distributional results, several Bayesian estimators for the model parameters are suggested along with their individual/joint credible intervals. We then explore the Bayesian design optimization under various design criteria based on Shannon information gain and the posterior variance-covariance matrix. Through Monte Carlo simulations, the performance of our proposed inferential methods are assessed and compared between the continuous and interval inspections. Finally, a real engineering case study for analyzing the reliability of a solar lighting device is presented to illustrate the methods developed in this work.

Key Words: accelerated life tests, Bayesian analysis, design of experiments, order-restricted inference, progressive Type-I censoring, step-stress loading

1. Introduction

Accelerated life testing (ALT) has become a familiar technique to expedite a life test. This design is valuable to reliability experiments because many products and devices nowadays are lasting longer. By adding stress to an experiment, say in the form of increased temperature, voltage or use in general, failures can be observed faster. This additional stress can be imposed in various ways. It can be constant, progressive (ramp) or added stepwise. To relate the results back to normal use conditions, one can use extrapolation.

Stress added stepwise is referred to as a step-stress accelerated life test (SSALT). Between these steps, the stress can be increased or decreased. This is called a simple SSALT when only two levels are considered. For typical parametric analysis of this data, each stress level is assumed to belong to some right-skewed distribution. To combine these different lifetime distributions, another assumption is made about the model that relates them. Commonly used models include the cumulative exposure (CE) model, see Nelson (1980), the tampered failure (TF) model, see Bhattacharyya and Soejoeti (1989), the tampered random variable (TRV) model, see DeGroot and Goel (1979) and the cumulative risk (CR) model, see van Dorp et al. (1996).

The CE model is popular because it is conceptually plausible. The main idea is that the distribution function can be constructed piecewise by bringing together the corresponding segments of the distributions of the different stress levels. There are instances where the CE model is equivalent to the TF and/or TRV models, for instance when the lifetime distributions are assumed to be exponential. This finding as well as a brief review and comparison of models is provided in Xu and Fei (2012).

*Department of Management Science and Statistics, University of Texas at San Antonio, One UTSA Circle, San Antonio, Texas 78249

†Department of Management Science and Statistics, University of Texas at San Antonio, One UTSA Circle, San Antonio, Texas 78249

When designing an experiment, various censoring schemes may be considered. To save resources, one might consider progressive censoring, which allows for items to be censored before the end of the experiment, such as at the stress change time point(s). Other considerations related to censoring include whether to use Type-I, Type-II or a hybrid censoring scheme. These choices depend on experimental constraints and goals. For more details on censoring schemes particularly related to SSALTs see Kundu and Ganguly (2017).

In the work to follow, we explore progressively Type-I censored simple SSALTs under continuous inspections assuming that the lifetimes are exponential and that a cumulative exposure model holds. The likelihood function for this then involves two (rate) parameters, λ_1 and λ_2. Intuitively we know that λ_1 should be less than λ_2. To impose this order restriction, we propose using a Bayesian framework with a three-parameter gamma ($viz.$, Erlang) distribution as a conditional prior. This prior results in a tractable joint posterior distribution, allowing for fairly quick computations.

Works related to order restricted inference include Balakrishnan et al. (2009), Ganguly et al. (2015), Samanta et al. (2017) and Mondal and Kundu (2020). The former work is approached in a Frequentist way while the latter three take a Bayesian approach. The Frequentist work is rather involved, obtaining estimates with the use of isotonic regression. The Bayesian estimates in the middle two noted works were obtained assuming that $\lambda_1 = \alpha\lambda_2$, where λ_2 follows a gamma distribution and α follows a beta distribution. This prior is understandable, yet leads to a posterior that does not have a closed form, requiring importance sampling. The last noted work explores Weibull lifetimes and uses a beta gamma prior to incorporate order restriction. This work too employs importance sampling to obtain estimates. In regards to design optimization, there are various references under these experimental settings, see for example Gouno et al. (2004), Wu et al. (2006) or Balakrishnan and Han (2009).

The goal of this article is to introduce a computationally more appealing Bayesian approach to order restricted simple SSALT inference and design optimization. This article is organized as follows. In Section 2 we provide the model for simple SSALTs under the previously mentioned Bayesian framework and assumptions. Additionally, we derive the joint and marginal posterior distributions and show how to obtain various estimators. In Section 3 we discuss the algorithms related to obtaining highest posterior density (HPD) credible regions. In Section 4 we discuss simulation results for Bayesian inference. In Section 5 we provide a real engineering case study for analyzing the reliability characteristic of a solar lighting device which illustrates the methods developed in this work. In Section 6 we discuss the results for Bayesian optimal design. And lastly, in Section 7 we conclude the paper and note our plans for future work.

2. Model Description

The model to follow is for simple step-stress accelerated life testing with progressive Type-I censoring under continuous monitoring. The assumptions are that a cumulative exposure model is appropriate and that the life distribution of a test unit is exponential at any level of stress. The likelihood function for this was given by Gouno et al. (2004). Using a rate parametrization, we have Equation 1. Here, n_i are the number of units that failed at the respective stress level x_i, i.e.) the number of failures observed in the time interval (τ_{i-1}, τ_i), and $U_i = \sum_{j=1}^{n_i}(t_{i,j} - \tau_{i-1}) + (N_i - n_i)(\tau_i - \tau_{i-1})$. N_i are the number of units entering at the respective stress level which depend on the the censoring proportion π^*.

$$L(\lambda_1, \lambda_2|\boldsymbol{t}) = \lambda_1^{n_1}\lambda_2^{n_2}\exp(-\lambda_1 U_1 - \lambda_2 U_2) \tag{1}$$

Using a Bayesian framework we propose an order restricted conjugate-like prior, $\pi(\lambda_1, \lambda_2)$,

that is a joint distribution of 3-parameter gamma ($viz.$, Erlang) distributions as in Equation 2. Utilizing the shift parameter in this distribution allows us to ensure that the rate parameter increases as the stress level increases.

$$\begin{aligned}
&\pi(\lambda_1) = \frac{\gamma_1^{\alpha_1}}{(\alpha_1-1)!}(\lambda_1)^{\alpha_1-1}\exp(-\gamma_1\lambda_1) \\
&\pi(\lambda_2|\lambda_1) = \frac{\gamma_2^{\alpha_2}}{(\alpha_2-1)!}(\lambda_2-\lambda_1)^{\alpha_2-1}\exp(-\gamma_2(\lambda_2-\lambda_1)) \\
&\alpha_i \in \{1,2,3,...\} \text{ and } \gamma_i > 0 \qquad i = 1,2.
\end{aligned} \tag{2}$$

To derive the exact joint posterior distribution, $\pi(\lambda_1, \lambda_2|\boldsymbol{t})$, we compute the following.

$$\begin{aligned}
\pi(\lambda_1,\lambda_2|\boldsymbol{t}) &\propto L(\lambda_1,\lambda_2|\boldsymbol{t})\pi(\lambda_1,\lambda_2) \\
&\propto L(\lambda_1,\lambda_2|\boldsymbol{t})\pi(\lambda_1)\pi(\lambda_2|\lambda_1) \\
&\propto \lambda_1^{n_1}\lambda_2^{n_2}\exp(-\lambda_1U_1-\lambda_2U_2)(\lambda_1)^{\alpha_1-1}\exp(-\gamma_1\lambda_1)(\lambda_2-\lambda_1)^{\alpha_2-1}\exp(-\gamma_2(\lambda_2-\lambda_1)) \\
&\propto \lambda_1^{n_1}\lambda_2^{n_2}\exp(-\lambda_1U_1-\lambda_2U_2)(\lambda_1)^{\alpha_1-1}\exp(-\gamma_1\lambda_1) \\
&\quad \times \sum_{j_1=0}^{\alpha_2-1}\binom{\alpha_2-1}{j_1}\lambda_2^{\alpha_2-1-j_1}(-1)^{j_1}(\lambda_1)^{j_1}\exp(-\gamma_2(\lambda_2-\lambda_1)) \\
&\propto \sum_{j_1=0}^{\alpha_2-1}\binom{\alpha_2-1}{j_1}(-1)^{j_1}\lambda_1^{n_1+\alpha_1+j_1-1}\exp(-\lambda_1(U_1+\gamma_1-\gamma_2)) \\
&\quad \times\lambda_2^{n_2+\alpha_2-j_1-1}\exp(-\lambda_2(U_2+\gamma_2))
\end{aligned} \tag{3}$$

What we see is that this computation results in a joint posterior distribution that is a generalized mixture of gamma densities. We use the result of (3) to compute a normalizing constant, which is shown in (4). Further, the marginal distributions, $\pi(\lambda_1|\boldsymbol{t})$ and $\pi(\lambda_2|\boldsymbol{t})$, are derived and given respectively in (5) and (6).

$$NC = \sum_{d=0}^{n_2}\binom{n_2}{d}\frac{\Gamma(\alpha_2+d)}{(U_2+\gamma_2)^{\alpha_2+d}}\frac{\Gamma(\alpha_1+n_1+n_2-d)}{(U_1+U_2+\gamma_1)^{\alpha_1+n_1+n_2-d}} \tag{4}$$

$$\pi(\lambda_1|\boldsymbol{t}) = NC^{-1}\sum_{i=0}^{n_2}\binom{n_2}{i}\frac{\Gamma(\alpha_2+i)}{(U_2+\gamma_2)^{\alpha_2+i}}\lambda_1^{n_1+n_2+\alpha_1-i-1}\exp(-\lambda_1(U_1+U_2+\gamma_1)) \tag{5}$$

$$\begin{aligned}
\pi(\lambda_2|\boldsymbol{t}) &= NC^{-1}\sum_{i=0}^{\alpha_2-1}\binom{\alpha_2-1}{i}(-1)^i\lambda_2^{n_2+\alpha_2-i-1}\exp(-\lambda_2(U_2+\gamma_2)) \\
&\quad \times\frac{(n_1+\alpha_1+i-1)!}{(U_1+\gamma_1-\gamma_2)^{n_1+\alpha_1+i}}\Big[1-\exp(-\lambda_2(U_1+\gamma_1-\gamma_2)) \\
&\quad \times\sum_{r=0}^{n_1+\alpha_1+i-1}\frac{(\lambda_2(U_1+\gamma_1-\gamma_2))^r}{r!}\Big]
\end{aligned} \tag{6}$$

To compute the marginal means and variances, we obtain the jth moments for both $\pi(\lambda_1|\boldsymbol{t})$ and $\pi(\lambda_2|\boldsymbol{t})$, which are shown in (7) and (8). The expectation of $(\lambda_1\lambda_2)$ computed from the joint posterior distribution is as shown in (9).

$$E(\lambda_1^j|\boldsymbol{t}) = \quad NC^{-1}\sum_{i=0}^{n_2}\binom{n_2}{i}\frac{\Gamma(\alpha_2+i)}{(U_2+\gamma_2)^{\alpha_2+i}}\frac{\Gamma(n_1+n_2+\alpha_1-i+j)}{(U_1+U_2+\gamma_1)^{n_1+n_2+\alpha_1-i+j}} \tag{7}$$

$$\begin{aligned} E(\lambda_2^j|\boldsymbol{t}) \quad = \quad & NC^{-1}\sum_{i=0}^{\alpha_2-1}\binom{\alpha_2-1}{i}(-1)^i\frac{(n_1+\alpha_1+i-1)!}{(U_1+\gamma_1-\gamma_2)^{n_1+\alpha_1+i}}\Big[\frac{\Gamma(n_2+\alpha_2-i+j)}{(U_2+\gamma_2)^{n_2+\alpha_2-i+j}} - \\ & \sum_{r=0}^{n_1+\alpha_1+i-1}\frac{(U_1+\gamma_1-\gamma_2)^r}{r!}\frac{\Gamma(n_2+\alpha_2-i+r+j)}{(U_1+U_2+\gamma_1)^{n_2+\alpha_2-i+r+j}}\Big] \end{aligned} \tag{8}$$

$$E(\lambda_1\lambda_2|\boldsymbol{t}) = \quad NC^{-1}\sum_{i=0}^{n_2+1}\binom{n_2+1}{i}\frac{\Gamma(\alpha_2+i)}{(U_2+\gamma_2)^{\alpha_2+i}}\frac{\Gamma(\alpha_1+n_1+n_2-i+2)}{(U_1+U_2+\gamma_1)^{\alpha_1+n_1+n_2-i+2}} \tag{9}$$

Additionally, we derived expressions for the marginal cumulative distribution functions (cdfs) to identify the quantiles including the median.

3. Credible Regions

To compute the joint credible region for (λ_1, λ_2), methodology adapted from Turkkan and Pham-Gia (1997) was used, see Algorithm 1. Here (L_1, U_1) and (L_2, U_2) represent the rectangular boundary of the contour at k (some density). Though the integration is performed to account for the constraint $\lambda_1 < \lambda_2$, this approach to compute the volume can still result in overestimation. The magnitude of this deviation is based on the shape of the posterior. Therefore, an alternative approach is to compute the volume using a mesh grid over the region instead. In the multimodal case, we recommend the grid. For the simulations in Section 4, a grid was used afterwards to estimate the actual volume.

Two approaches are proposed to compute the marginal credible intervals. In a similar fashion as to the joint interval, one approach is to compute the area of the distribution at a given density. The proposed starting point is at some ϵ value just below the mode. At this density, the intersecting points of the distribution, can be computed using a root finding technique. The corresponding area is then obtained using the respective cdfs. We can continue to travel down the density until the desired area is achieved.

For the case when the marginal distribution is multimodal, a sliding window approach should be considered. Here, starting at $l = 0$, we can identify the value, u, at which the desired area under the curve is obtained. Then incrementing by some small ϵ value, we compute the respective u values. The credible interval will be the (l, u) with the shortest length.

Algorithm 1 Construction of the $100(1-\alpha)\%$ HPD Joint Credible Region for (λ_1, λ_2)

$k \leftarrow \max\{\pi(\lambda_1, \lambda_2|\boldsymbol{t})\}$
while $k > 0$ **do**
$\mathcal{S} \leftarrow \{(\lambda_1, \lambda_2) \mid \pi(\lambda_1, \lambda_2|\boldsymbol{t}) = k\}$
$L_1 \leftarrow \min\left\{ \binom{1}{0}^T v \;\middle|\; v \in \mathcal{S} \right\}$ and $U_1 \leftarrow \max\left\{ \binom{1}{0}^T v \;\middle|\; v \in \mathcal{S} \right\}$
$L_2 \leftarrow \min\left\{ \binom{0}{1}^T v \;\middle|\; v \in \mathcal{S} \right\}$ and $U_2 \leftarrow \max\left\{ \binom{0}{1}^T v \;\middle|\; v \in \mathcal{S} \right\}$
$M \leftarrow \max\{U_1, L_2\}$

$$\text{Volume} \leftarrow \int_{L_2}^{U_2}\int_{L_1}^{U_1} \pi(\lambda_1, \lambda_2|\mathbf{t})d\lambda_1 d\lambda_2 = \int_{L_2}^{M}\int_{L_1}^{\lambda_2} \pi(\lambda_1, \lambda_2|\mathbf{t})d\lambda_1 d\lambda_2 + \int_{M}^{U_2}\int_{L_1}^{U_1} \pi(\lambda_1, \lambda_2|\mathbf{t})d\lambda_1 d\lambda_2$$

if Volume = 1-α **then**
break
else
$k \leftarrow k - \epsilon$
end if
end while
return $[L_1, U_1;\ L_2, U_2]$

4. Simulation Results

A Monte Carlo simulation study was conducted with the parameter values $\lambda_1 = 1.1052$ and $\lambda_2 = 2.7183$ along with the hyperparameters $\alpha_1 = \alpha_2 = 2$, $\gamma_1 = \gamma_2 = 0.001$ and then $\gamma_1 = \gamma_2 = 0.0001$. The selections made for λ_1 and λ_2 were motivated by the desire to follow choices made for related frequentist work of Han and Bai (2020). The specific choices of hyperparameters α_1, α_2, γ_1, and γ_2 were explored in order to make the joint prior distribution as noninformative/objective as possible. The integer-valued shape hyperparameters only allow for a limited number of options. Setting $\alpha_1 = \alpha_2 = 5$ was considered; however, for the given sample sizes, this prior was overpowering and exhibited a more drastic and negative impact on the inference for λ_1 and λ_2, yielding unsatisfactory results by severely overestimating λ_2. On the other hand, sensitivity analyses revealed negligible impact on all the measures considered in this study when changing the rate hyperparameters between $\gamma_1 = \gamma_2 = 0.001$ and $\gamma_1 = \gamma_2 = 0.0001$. The results to follow are based off of 1000 simulations with $n = 24$ and then repeated for $n = 48$. As an illustration, equal step durations were implemented with the total test duration choices of $\tau = 0.9$, $\tau = 1.2$ and $\tau = 1.5$. Given the progressive Type-I censoring scheme, the proportion of surviving units to censor after the first level was chosen as $\pi^* = 0\%$, $\pi^* = 10\%$ and $\pi^* = 20\%$.

Bayesian estimators for the model parameters λ_1 and λ_2 include the means, medians and modes from the respective marginal distributions. From Tables 1 and 2, it is observed that for both λ_1 and λ_2, the posterior mean $>$ the posterior median $>$ the posterior mode, indicating that each marginal posterior is skewed to the right as expected from a mixture of gamma densities. In all simulations, these values overestimate the selected parameter values for the study, primarily due to the choice of our priors having positive means. Such deviation is more pronounced for λ_2 with much larger posterior variance than for λ_1. This relatively poor performance for estimation of λ_2 is not always the case but because of the

particular experimental setup chosen for our simulation study with equal durations at the two stress levels. As the sample size n increases from 24 to 48, we see that all Bayes estimates (posterior mean, median, and mode) for λ_1 and λ_2 decrease towards the specified value of each parameter, especially in a larger degree for λ_2; see Tables 1 and 2. The posterior variance of λ_1 exhibits almost 50% reduction while that of λ_2 shows reduction between 50% to 65%, depending on other parameter values. The posterior covariance between λ_1 and λ_2 also decreases substantially, making these parameters less correlated with a larger sample size. It is understood that an increase of the sample size diminishes the relative impact of the joint prior which originally models a moderately strong positive correlation of 0.7071 between the parameters based on the conditional three-parameter gamma distribution.

The 95% HPD credible intervals for λ_1 and λ_2 are presented in Tables 3 and 4 based on their marginal posterior distributions as well as in Tables 5 and 6 based on their joint posterior. In the case of λ_1, for all selections, roughly 95% of intervals contain the selected value; however, such results are not obtained for λ_2, with 90-94% of intervals containing the selected value, depending on choices of n, τ and π^*. Also, in general, λ_2 has a much larger posterior variance than λ_1, as demonstrated in Tables 1 and 2, resulting in much wider marginal HPD credible intervals for λ_2. An interesting observation here is that a wider credible interval for λ_2 on average does not necessarily improve the percentage of intervals containing its selected value. It is because a larger average interval length for λ_2 is associated with not only a larger posterior variance but also further overestimation of λ_2 due to its upward biased mode and right-skewed posterior. As n increases, the marginal 95% HPD credible intervals all shrink for both parameters. For λ_1, the interval widths are decreased by 30% on average while the degree of shrinkage is a little more substantial for λ_2. As aforementioned, for λ_1, the proportion of intervals containing the selected value is consistently higher than 95% while it is consistently lower for λ_2. With an increased sample size, it is observed that both proportions improve, getting closer to the 95% level. The magnitude of improvement is more noticeable for λ_2 than for λ_1.

With a larger n, the joint 95% HPD credible regions also get tightened while the coverage proportion improves. It is noticed that for each parameter, the upper bound of the marginal intervals and joint regions shrinks faster to the center than the corresponding lower bound as the sample size increases. This is because with an increased sample size, our (extremely dispersed) relatively objective prior has less influence on the posterior, reducing the overall right skewness of the posterior more drastically. Algorithm 1 described in the previous section provides a simplified approach to compute the joint credible region presented in Tables 5 and 6. Using this algorithm establishes a rectangular or polygon region around the joint distribution, and thus, the actual volume of the posterior inside the region is potentially underestimated. To quantify this, a mesh grid for the cross section of the joint posterior enclosed by the region was used to better estimate the actual volume/probability. As expected, the actual coverage proportion of the joint 95% HPD credible region proposed in this study is slightly less than the nominal but reasonable as it consistently achieves about 92% on average regardless of other parameter values. To improve this coverage proportion without hurting the computational efficiency, one may slightly enlarge the joint credible region by proportionately expanding the distance of each side of the rectangle from the location of the posterior mode.

It is also observed from Tables 1 through 4 that increasing π^*, the proportion of intermediate censoring, increases both the variances and average interval lengths for λ_1 and λ_2. This is exactly the opposite effect of increasing the sample size n since censoring reduces the effective sample size and thus the amount of information from an ALT experiment. With these observations, we see that a larger sample size and a smaller proportion of surviving

units to censor result in better estimates, especially for λ_2. To further improve estimates of λ_2, another consideration would be to use unequal step durations, such as short first level and long second level.

As the total test duration τ increases, all Bayes estimates for λ_1 decrease while those for λ_2 all increase. At the same time, the posterior variance of λ_1 decreases while the posterior variance of λ_2 increases. In turn, the average lengths of the corresponding marginal HPD credible intervals for λ_1 and λ_2 respectively decrease and increase. A similar trend is also observed for their joint HPD credible regions in Tables 5 and 6. The range of λ_1 decreases as a function of τ while that of λ_2 increases. Again, this observation is due to the particular experimental scenario chosen for the simulation study with uniform durations at the two stress levels. With a longer test duration τ, the probability of collecting more failures, or equivalently more information, at the first stress level x_1 gets higher. This has an obvious effect of improving the estimates of λ_1, reducing its dispersion. However, this results in cutting down the number of surviving test units to enter the second stress level x_2. This trade-off reduces the amount of information available to estimate λ_2, hence blowing up its dispersion and worsening the estimation precision. Using 1000 samples, each of the size $n = 24$ under conventional Type-I censoring, we compared the number of failures observed at each stress level for $\tau = 0.90$ and $\tau = 1.50$. Respectively, for this change in τ, the mean number of failures observed in the first stress level jumps from 9.244 to 13.346 while dropping from 10.440 to 9.264 for the second stress level. Under progressive censoring with $\pi^* = 0.20$, there are even fewer failures observed at the second stress level, averages of 8.355 and 7.424. Regardless of the marginal estimations, a longer test duration eventually provides a better chance to collect more failure data, improving the overall information quality. This translates to less relative influence of the prior on the posterior, and it is reflected in the posterior covariance between λ_1 and λ_2 decreasing with increasing τ as shown in Tables 1 and 2.

As stated earlier, based on the sensitivity analyses to the hyperparameters, a negligible impact was observed on all the measures considered in this study when changing the rate hyperparameters γ_1 and γ_2 of the joint prior of λ_1 and λ_2. On the contrary, the shape hyperparameters α_1 and α_2 of the joint prior have exhibited more drastic and negative impact on the inference for λ_1 and λ_2. Increasing these shape hyperparameters can blow up the uncertainty around λ_1 and λ_2 as well as the magnitude of overestimation. In order to compensate for this concern about large shape hyperparameters, one should secure a budget to accommodate a very large sample size in practice. From the computational viewpoint, large shape hyperparameters are also troublesome as they require more iterative sum operations for calculation of the posterior distribution, tending to accumulate numerical errors more rapidly. Without strong prior knowledge and/or preference on these shape hyperparameters, it is therefore recommended to choose smaller shape hyperparameters in practice in order to enhance both inferential and computational performances.

5. Illustrative Example

Using the described Bayesian framework, inference for the simple step-stress test data of solar lighting devices as seen in Han and Kundu (2015) was conducted. In the solar lighting device dataset, the stress factor was temperature, which was noted to typically operate at 293K but was ramped up to 353K for the study. For this illustration, the two failure modes of the device were ignored. The stress was changed at $\tau_1 = 5$ (hundred hours) and Type-I censoring occurred at $\tau_2 = 6$ (hundred hours). For the first stress level, there were $n_1 = 16$ failures and for the second stress level, there were $n_2 = 15$ failures; 4 observations were right censored.

Table 1: Marginal Simulation Results for n = 24, $\alpha_1 = \alpha_2 = 2$, $\gamma_1 = \gamma_2 = \gamma$

			λ_1				λ_2				
γ	τ	π^*	Mean	Median	Mode	Variance	Mean	Median	Mode	Variance	Covariance
0.0001	0.9	0%	1.240	1.207	1.140	0.131	3.681	3.587	3.395	0.993	0.042
		10%	1.242	1.209	1.142	0.132	3.788	3.682	3.468	1.143	0.044
		20%	1.245	1.211	1.143	0.133	3.913	3.794	3.552	1.363	0.047
	1.2	0%	1.220	1.192	1.136	0.108	3.766	3.664	3.458	1.134	0.034
		10%	1.221	1.194	1.137	0.108	3.871	3.758	3.528	1.358	0.036
		20%	1.223	1.195	1.138	0.109	4.008	3.880	3.619	1.597	0.038
	1.5	0%	1.210	1.186	1.136	0.093	3.887	3.772	3.539	1.420	0.031
		10%	1.212	1.188	1.138	0.094	4.035	3.906	3.644	1.711	0.032
		20%	1.214	1.189	1.139	0.095	4.182	4.037	3.742	2.023	0.035
0.0010	0.9	0%	1.240	1.207	1.140	0.131	3.680	3.586	3.394	0.993	0.042
		10%	1.242	1.209	1.142	0.132	3.787	3.681	3.467	1.142	0.044
		20%	1.245	1.211	1.143	0.133	3.912	3.793	3.551	1.362	0.047
	1.2	0%	1.220	1.192	1.136	0.108	3.765	3.663	3.457	1.133	0.034
		10%	1.221	1.194	1.137	0.108	3.870	3.757	3.527	1.356	0.036
		20%	1.223	1.195	1.138	0.109	4.006	3.878	3.618	1.596	0.038
	1.5	0%	1.210	1.186	1.136	0.093	3.886	3.771	3.538	1.418	0.031
		10%	1.212	1.188	1.138	0.094	4.033	3.905	3.642	1.709	0.032
		20%	1.214	1.189	1.139	0.095	4.181	4.036	3.740	2.020	0.035

Table 2: Marginal Simulation Results for n = 48, $\alpha_1 = \alpha_2 = 2$, $\gamma_1 = \gamma_2 = \gamma$

			λ_1				λ_2				
γ	τ	π^*	Mean	Median	Mode	Variance	Mean	Median	Mode	Variance	Covariance
0.0001	0.9	0%	1.179	1.161	1.126	0.065	3.167	3.121	3.026	0.412	0.012
		10%	1.179	1.162	1.127	0.065	3.209	3.157	3.052	0.463	0.013
		20%	1.180	1.163	1.127	0.065	3.268	3.210	3.091	0.531	0.014
	1.2	0%	1.171	1.156	1.127	0.053	3.197	3.148	3.049	0.441	0.010
		10%	1.171	1.156	1.127	0.053	3.251	3.196	3.086	0.498	0.011
		20%	1.171	1.157	1.127	0.053	3.306	3.244	3.119	0.574	0.012
	1.5	0%	1.164	1.152	1.126	0.046	3.263	3.208	3.098	0.505	0.009
		10%	1.165	1.152	1.126	0.046	3.328	3.267	3.144	0.577	0.010
		20%	1.165	1.152	1.127	0.046	3.403	3.334	3.195	0.668	0.010
0.0010	0.9	0%	1.179	1.161	1.126	0.065	3.167	3.120	3.026	0.412	0.012
		10%	1.179	1.162	1.127	0.065	3.209	3.157	3.052	0.463	0.013
		20%	1.180	1.163	1.127	0.065	3.268	3.209	3.090	0.531	0.014
	1.2	0%	1.171	1.156	1.127	0.053	3.197	3.148	3.048	0.441	0.010
		10%	1.171	1.156	1.127	0.053	3.250	3.196	3.085	0.498	0.011
		20%	1.171	1.157	1.127	0.053	3.305	3.244	3.118	0.574	0.012
	1.5	0%	1.164	1.152	1.126	0.046	3.262	3.208	3.098	0.504	0.009
		10%	1.165	1.152	1.126	0.046	3.327	3.267	3.143	0.577	0.010
		20%	1.165	1.152	1.127	0.046	3.402	3.334	3.194	0.668	0.010

Using hyperparameters $\alpha_1 = \alpha_2 = 2$ and $\gamma_1 = \gamma_2 = 0.001$, the observed reliability characteristics of a solar lighting device included the values provided in Table 7. The boundaries of the joint credible region for (λ_1, λ_2) as described in Section 3 were found to be $(0.0686184, 0.2059834)$ and $(1.058771, 3.271246)$. This rectangular region is depicted in Figure 1. This volume is estimated to be roughly 92%. Marginal credible intervals were obtained as $(0.074376, 0.194507)$ and $(1.150563, 3.085970)$.

Table 3: Marginal Credible Intervals for n = 24, $\alpha_1 = \alpha_2 = 2$, $\gamma_1 = \gamma_2 = \gamma$

			λ_1			λ_2		
γ	τ	π^*	95% Interval	Width	Cover %	95% Interval	Width	Cover %
0.0001	0.9	0%	(0.588, 1.950)	1.362	95.7%	(1.940, 5.594)	3.653	91.7%
		10%	(0.588, 1.955)	1.367	95.6%	(1.933, 5.835)	3.902	91.5%
		20%	(0.588, 1.961)	1.372	95.6%	(1.925, 6.120)	4.196	91.2%
	1.2	0%	(0.624, 1.864)	1.240	95.1%	(1.950, 5.766)	3.816	92.1%
		10%	(0.625, 1.867)	1.242	95.3%	(1.939, 6.010)	4.071	91.7%
		20%	(0.625, 1.870)	1.246	95.3%	(1.932, 6.319)	4.387	90.1%
	1.5	0%	(0.652, 1.811)	1.159	95.7%	(1.944, 6.039)	4.095	90.7%
		10%	(0.652, 1.815)	1.163	95.6%	(1.947, 6.359)	4.412	90.0%
		20%	(0.653, 1.818)	1.165	95.5%	(1.941, 6.692)	4.752	90.3%
0.0010	0.9	0%	(0.588, 1.950)	1.362	95.7%	(1.940, 5.592)	3.652	91.8%
		10%	(0.588, 1.955)	1.367	95.6%	(1.932, 5.833)	3.901	91.5%
		20%	(0.588, 1.961)	1.372	95.6%	(1.924, 6.118)	4.194	91.2%
	1.2	0%	(0.624, 1.864)	1.240	95.1%	(1.949, 5.764)	3.815	92.2%
		10%	(0.625, 1.867)	1.242	95.3%	(1.939, 6.008)	4.069	91.7%
		20%	(0.625, 1.870)	1.246	95.3%	(1.931, 6.317)	4.385	90.1%
	1.5	0%	(0.652, 1.811)	1.159	95.7%	(1.943, 6.037)	4.093	90.7%
		10%	(0.652, 1.815)	1.163	95.6%	(1.947, 6.357)	4.410	90.0%
		20%	(0.653, 1.818)	1.165	95.5%	(1.940, 6.689)	4.749	90.3%

Table 4: Marginal Credible Intervals for n = 48, $\alpha_1 = \alpha_2 = 2$, $\gamma_1 = \gamma_2 = \gamma$

			λ_1			λ_2		
γ	τ	π^*	95% Interval	Width	Cover %	95% Interval	Width	Cover %
0.0001	0.9	0%	(0.706, 1.682)	0.976	95.1%	(1.992, 4.424)	2.432	93.9%
		10%	(0.706, 1.683)	0.977	95.2%	(1.969, 4.540)	2.571	93.5%
		20%	(0.706, 1.685)	0.979	94.8%	(1.948, 4.691)	2.743	93.7%
	1.2	0%	(0.740, 1.626)	0.885	95.0%	(1.988, 4.492)	2.503	93.0%
		10%	(0.740, 1.626)	0.886	94.7%	(1.973, 4.624)	2.650	92.7%
		20%	(0.740, 1.627)	0.887	94.6%	(1.947, 4.773)	2.826	93.7%
	1.5	0%	(0.762, 1.588)	0.825	95.7%	(1.984, 4.637)	2.653	92.6%
		10%	(0.762, 1.588)	0.826	95.6%	(1.971, 4.791)	2.819	92.0%
		20%	(0.762, 1.589)	0.827	95.6%	(1.954, 4.972)	3.018	91.4%
0.0010	0.9	0%	(0.706, 1.682)	0.976	95.1%	(1.991, 4.423)	2.432	93.9%
		10%	(0.706, 1.683)	0.977	95.2%	(1.969, 4.539)	2.570	93.5%
		20%	(0.706, 1.685)	0.979	94.8%	(1.948, 4.690)	2.743	93.8%
	1.2	0%	(0.740, 1.626)	0.885	95.0%	(1.988, 4.491)	2.503	93.0%
		10%	(0.740, 1.626)	0.886	94.7%	(1.973, 4.623)	2.650	92.8%
		20%	(0.740, 1.627)	0.887	94.6%	(1.947, 4.772)	2.825	93.7%
	1.5	0%	(0.762, 1.588)	0.825	95.7%	(1.983, 4.636)	2.653	92.6%
		10%	(0.762, 1.588)	0.826	95.6%	(1.971, 4.790)	2.819	92.0%
		20%	(0.762, 1.589)	0.827	95.6%	(1.954, 4.971)	3.017	91.4%

6. Design Optimization

For design optimization, the hyperparameters of the prior as seen in Equation 2 were set as $\alpha_1 = \alpha_2 = 2$, $\gamma_1 = 1.809675$ and $\gamma_2 = 1.23984$. These selections were made to make the

Table 5: Joint Credible Intervals for n = 24, $\alpha_1 = \alpha_2 = 2$, $\gamma_1 = \gamma_2 = \gamma$

			95% Joint HPD Credible Region			
γ	τ	π^*	Range of λ_1	Range of λ_2	Joint Cover %	Actual Volume
0.0001	0.9	0%	(0.534, 2.099)	(1.728, 5.903)	93.6%	91.9%
		10%	(0.534, 2.105)	(1.712, 6.171)	93.8%	91.9%
		20%	(0.534, 2.112)	(1.692, 6.490)	94.2%	91.9%
	1.2	0%	(0.572, 1.994)	(1.741, 6.104)	93.4%	91.8%
		10%	(0.572, 1.998)	(1.722, 6.377)	92.9%	91.8%
		20%	(0.572, 2.003)	(1.704, 6.722)	92.4%	91.9%
	1.5	0%	(0.601, 1.931)	(1.732, 6.415)	92.2%	91.8%
		10%	(0.601, 1.935)	(1.725, 6.772)	91.7%	91.8%
		20%	(0.601, 1.939)	(1.709, 7.144)	91.4%	91.8%
0.0010	0.9	0%	(0.534, 2.099)	(1.728, 5.901)	93.6%	91.9%
		10%	(0.534, 2.105)	(1.711, 6.170)	93.8%	91.9%
		20%	(0.534, 2.111)	(1.692, 6.487)	94.2%	91.9%
	1.2	0%	(0.572, 1.994)	(1.741, 6.102)	93.4%	91.8%
		10%	(0.572, 1.998)	(1.721, 6.374)	92.9%	91.8%
		20%	(0.572, 2.002)	(1.703, 6.719)	92.4%	91.9%
	1.5	0%	(0.601, 1.930)	(1.731, 6.412)	92.2%	91.8%
		10%	(0.601, 1.935)	(1.725, 6.769)	91.7%	91.8%
		20%	(0.601, 1.938)	(1.708, 7.140)	91.4%	91.8%

Table 6: Joint Credible Intervals for n = 48, $\alpha_1 = \alpha_2 = 2$, $\gamma_1 = \gamma_2 = \gamma$

			95% Joint HPD Credible Region			
γ	τ	π^*	Range of λ_1	Range of λ_2	Joint Cover %	Actual Volume
0.0001	0.9	0%	(0.660, 1.776)	(1.851, 4.629)	94.3%	91.8%
		10%	(0.660, 1.777)	(1.823, 4.759)	94.4%	91.8%
		20%	(0.660, 1.779)	(1.794, 4.929)	94.6%	91.8%
	1.2	0%	(0.697, 1.709)	(1.848, 4.708)	93.8%	91.8%
		10%	(0.697, 1.710)	(1.827, 4.856)	93.7%	91.8%
		20%	(0.697, 1.710)	(1.794, 5.024)	93.4%	91.8%
	1.5	0%	(0.721, 1.664)	(1.840, 4.872)	94.2%	91.8%
		10%	(0.721, 1.665)	(1.821, 5.044)	93.1%	91.8%
		20%	(0.721, 1.666)	(1.797, 5.246)	93.5%	91.8%
0.0010	0.9	0%	(0.660, 1.776)	(1.851, 4.629)	94.3%	91.8%
		10%	(0.660, 1.777)	(1.822, 4.759)	94.4%	91.8%
		20%	(0.660, 1.779)	(1.794, 4.928)	94.6%	91.8%
	1.2	0%	(0.697, 1.709)	(1.848, 4.708)	93.9%	91.8%
		10%	(0.697, 1.710)	(1.827, 4.855)	93.7%	91.8%
		20%	(0.697, 1.710)	(1.794, 5.023)	93.4%	91.8%
	1.5	0%	(0.721, 1.664)	(1.840, 4.871)	94.2%	91.8%
		10%	(0.721, 1.665)	(1.821, 5.043)	93.1%	91.8%
		20%	(0.721, 1.666)	(1.797, 5.246)	93.5%	91.8%

prior distribution informative and to also follow choices made for the related Frequentist work (Han and Bai, 2020). In addition to considering rate parameterizations, we also used

Table 7: Solar Lighting Device Results for n = 35, $\alpha_1 = \alpha_2 = 2$, $\gamma_1 = \gamma_2 = 0.001$

λ_1				λ_2				
Mean	Median	Mode	Variance	Mean	Median	Mode	Variance	Covariance
0.132	0.130	0.125	0.001	2.083	2.042	1.961	0.253	0.000

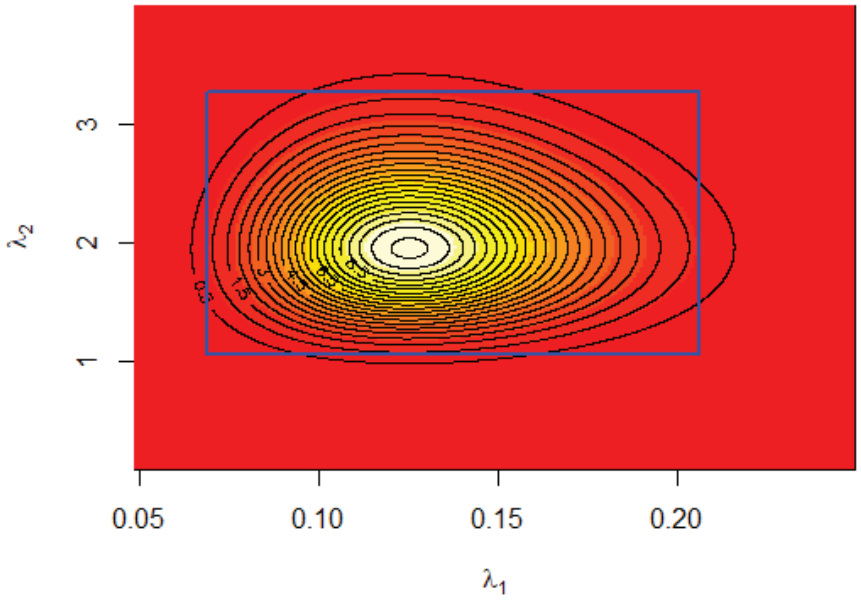

Figure 1: Contour Plot of $\pi(\lambda_1, \lambda_2|\boldsymbol{t})$ for the Solar Light Data

a linear link to express the exponential rate parameters as a regression function of the stress level, specifically $\lambda_i = \beta_0 + \beta_1 x_i$. The stress level settings were $x_1 = 0.1$ and $x_2 = 1$.

The design criteria explored included an information theoretic consideration, H-optimality, as well as various criteria based on the posterior variance-covariance matrix for both $\boldsymbol{\lambda}$ and $\boldsymbol{\beta}$, optimality designs A, C, D, E and M. H-optimality was defined as the value that maximizes the utility function $U_H(\cdot)$, the expected information gain based on the posterior entropy as in Lindley (1956).

$$U_H(\cdot) = E_{\boldsymbol{t}}[\int \pi(\boldsymbol{\lambda}|\boldsymbol{t}) \log \pi(\boldsymbol{\lambda}|\boldsymbol{t}) d\boldsymbol{\lambda} - \int \pi(\boldsymbol{\lambda}) \log \pi(\boldsymbol{\lambda}) d\boldsymbol{\lambda}]$$

A, C, D, E and M optimality designs are modified versions of those known under the Frequentist setting. Specific adjustments were made to conform the ranges of the utility functions to $\mathbb{R}$. Where V is the posterior variance-covariance matrix, these functions are defined as follows:

$$
\begin{aligned}
U_A(\cdot) &= E[-\log tr(V)] \\
U_C(\cdot) &= E[-\log V_{\boldsymbol{\beta}}[1,1]] \\
U_D(\cdot) &= E[-\log det(V)] \\
U_E(\cdot) &= E[-\log max \text{ eigenvalue}(V)] \\
U_M(\cdot) &= E[-\log max(V[1,1], V[2,2])]
\end{aligned}
$$

A-optimality was then identified as the value that maximizes $U_A(\cdot)$, the expected negative log of the the trace of the posterior variance-covariance matrix. C-optimality was identified as the value that maximizes $U_C(\cdot)$, the expected negative log of the posterior variance at normal operating conditions, the first element in Equation 10. D-optimality criteria was identified as the value that maximizes $U_D(\cdot)$, the expected negative log of the determinant of the posterior variance-covariance matrix. E-optimality criteria was identified as the value that maximizes $U_E(\cdot)$, the expected negative log of the maximum eigenvalue of the posterior variance-covariance matrix. Lastly, M-optimality criteria was identified as the value that maximizes $U_M(\cdot)$, the expected negative log of the maximum posterior variance.

The posterior variance-covariance matrix of $\boldsymbol{\beta}$ is given as:

$$
\mathrm{V}_{\boldsymbol{\beta}} = \begin{pmatrix} \frac{x_1^2 \mathrm{v}(\lambda_2|\boldsymbol{t}) + x_2^2 \mathrm{v}(\lambda_1|\boldsymbol{t}) - 2x_1x_2\mathrm{c}(\lambda_1,\lambda_2|\boldsymbol{t})}{(x_2-x_1)^2} & \frac{-x_1x_2}{(x_2-x_1)^2}\left[\frac{\mathrm{v}(\lambda_1|\boldsymbol{t})}{x1} - (\frac{1}{x_1}+\frac{1}{x_2})\mathrm{c}(\lambda_1,\lambda_2|\boldsymbol{t}) + \frac{\mathrm{v}(\lambda_2|\boldsymbol{t})}{x2}\right] \\ \frac{-x_1x_2}{(x_2-x_1)^2}\left[\frac{\mathrm{v}(\lambda_1|\boldsymbol{t})}{x1} - (\frac{1}{x_1}+\frac{1}{x_2})\mathrm{c}(\lambda_1,\lambda_2|\boldsymbol{t}) + \frac{\mathrm{v}(\lambda_2|\boldsymbol{t})}{x2}\right] & \frac{\mathrm{v}(\lambda_2|\boldsymbol{t}) + \mathrm{v}(\lambda_1|\boldsymbol{t}) - 2\mathrm{c}(\lambda_1,\lambda_2|\boldsymbol{t})}{(x_2-x_1)^2} \end{pmatrix}. \tag{10}
$$

Here v(·) represents the variance and c(·) is the covariance. These values are obtained from using Equations 7, 8, and 9.

The results to follow are based off of $m = 1000$ simulations with $n = 24$ and then repeated for $n = 48$. Given the progressive Type-I censoring scheme, choices for the proportion of surviving units to censor after the first level were chosen as $\pi = 0\%$, $\pi = 10\%$ and $\pi = 20\%$. Only equal step durations were considered for this study. The results in Tables 8 and 9 show, Δ^*, the optimal values for τ (the total test duration), and U^*, the value of the utility function evaluated at Δ^*. Algorithm 2 was adapted from Hong et al. (2014) and shows the approach taken for the simulation of criteria related to the posterior variance-covariance matrix. For the last item in this algorithm, the `optimize` function from the software package `R` was used. Due to the stochastic nature of this simulation, various local minimums were observed. With this, we note that some optimality criteria results show curious patterns for Δ^* as π^* increases. After preparing these results, we noticed that most of the values of Δ^* for D-optimality were the same for both $\boldsymbol{\lambda}$ and $\boldsymbol{\beta}$. Mathematically the utility functions were found to be proportional to one another. For H-optimality, we used an additional 1000 samples for each of the 1000 simulated $\boldsymbol{\lambda}$ values. For each $\boldsymbol{\lambda_i}$ the log of the prior was computed as well as the mean of the log for the 1000 posteriors. The utility function was then computed as the difference in the mean of the mean of the log for the posteriors and the mean of the log for the priors.

Algorithm 2 Stochastic Algorithm

1. Simulate m samples of $\boldsymbol{\lambda}$ from the prior in Equation 2.
2. For each $\boldsymbol{\lambda_i}$, simulate n random samples of $\boldsymbol{t_i}$ from the likelihood in Equation 1.
3. For each $\boldsymbol{t_i}$, compute the posterior variance-covariance matrix V_i for $\boldsymbol{\lambda_i}$ (or $\boldsymbol{\beta_i}$ based on a linear link using that in 10).
4. Compute the value of a respective utility function $U(\Delta)$ by obtaining the mean of the simulated measures, $\sum_{i=1}^{m} g(V_i)/m$ with an appropriate transformation $g(\cdot)$.
5. Identify the value of Δ which maximizes $U(\Delta)$.

Table 8: Design Optimization Based on the Variance-Covariance Matrix of β_0 and β_1.

		D-optimality		C-optimality		A-optimality		M-optimality		E-optimality	
n	π^*	Δ^*	U^*	Δ^*	U^*	Δ^*	U^*	Δ^*	U^*	Δ^*	U^*
24	0%	2.42301	3.69274	7.84469	-0.10721	1.49730	0.54488	1.21766	0.72288	1.23000	0.68171
	10%	3.13124	3.64830	7.06943	-0.11295	1.32684	0.49567	1.09724	0.65724	1.24140	0.62389
	20%	3.27426	3.58631	7.91807	-0.12232	1.44988	0.43266	1.13214	0.59185	1.26578	0.55759
48	0%	2.31228	4.77175	6.17256	-0.25870	1.28886	1.02870	1.14192	1.19298	1.11259	1.14516
	10%	2.49016	4.70252	6.17522	-0.27149	1.37042	0.96781	1.06377	1.12625	0.98991	1.07539
	20%	2.29750	4.62478	5.26573	-0.28468	1.29105	0.90029	0.99203	1.04713	0.99090	1.00511

Table 9: Design Optimization Based on the Variance-Covariance Matrix of λ_1 and λ_2.

		H-optimality		D-optimality		A-optimality		M-optimality		E-optimality	
n	π^*	Δ^*	U^*	Δ^*	U^*	Δ^*	U^*	Δ^*	U^*	Δ^*	U^*
24	0%	3.18320	1.59285	2.42301	3.90346	1.24943	0.74869	1.24396	0.92023	1.24397	0.89607
	10%	3.00969	1.57049	3.13124	3.85902	1.34591	0.68594	1.24141	0.84956	1.24028	0.82618
	20%	3.77340	1.54362	3.27526	3.79654	1.38578	0.61774	1.12210	0.77392	1.24961	0.75272
48	0%	2.35778	2.09843	2.31228	4.98247	1.15106	1.27669	1.04426	1.44659	1.03553	1.42792
	10%	2.36064	2.06612	2.49016	4.91324	1.11147	1.20838	1.06364	1.36927	1.06662	1.35264
	20%	2.33393	2.02840	2.30025	4.83524	0.99187	1.12303	0.99186	1.28136	0.99091	1.26541

7. Conclusion

Using a 3-parameter gamma distribution as a conditional prior, we have performed Bayesian estimation and design optimization for progressively Type-I censored simple SSALTs under continuous inspections assuming that the lifetimes are exponential and that a cumulative exposure model holds. This prior ensures that the failure rates increase as the stress level increases. This prior leads to a tractable joint posterior distribution, which is a mixture of gamma densities.

Using hyperparameters that result in a relatively objective prior for inference, we noticed in our simulation study that the variability for estimates of λ_2 was quite high compared to that of λ_1 and that the coverage percentage was less than desired. This issue appears to be rectifiable though. A quick test using different durations for τ and another using an informative prior both showed better results for λ_2. Using hyperparameters that result in an

informative prior for design optimization, we are able to recommend values of τ, the total test duration, that can be used in test planning under various design criteria.

Our future work includes extending this framework to the interval monitoring setting and to explore different censoring schemes. Additionally, we are interested in extending this to the general k-level SSALT. In regards to design optimization, we would like to explore results for other criteria such as minimizing the variance of a target quantile and also to consider flexible/non-uniform stress durations.

REFERENCES

Balakrishnan, N., Beutner, E. and Kateri, M. (2009), "Order restricted inference for exponential step-stress models," *IEEE Transactions on Reliability*, 58, 132–142.

Balakrishnan, N. and Han, D. (2009), "Optimal step-stress testing for progressively Type-I censored data from exponential distribution," *Journal of Statistical Planning and Inference*, 139, 1782–1798.

Bhattacharyya, G.K. and Soejoeti, Z. (1989), "A tampered failure rate model for step-stress accelerated life test," *Communications in Statistics - Theory and Methods*, 18, 1627–1643.

DeGroot, M.H. and Goel, P.K. (1979), "Bayesian estimation and optimal designs in partially accelerated life testing," *Naval Research Logistics*, 26, 223–235.

Ganguly, A., Kundu, D. and Mitra, S. (2015), "Bayesian Analysis of a Simple Step-Stress Model Under Weibull Lifetimes," *IEEE Transactions on Reliability*, 64, 473–485.

Gouno, E., Sen, A. and Balakrishnan, N. (2004), "Optimal step-stress test under progressive Type-I censoring," *IEEE Transactions on Reliability*, 53, 388–393.

Han, D. and Bai, T. (2020), "Parameter estimation using EM algorithm for lifetimes from step-stress and constant-stress accelerated life tests with interval monitoring," *IEEE Transactions on Reliability* (in print).

Han, D. and Kundu, D. (2015), "Inference for a step-stress model with competing risks for failure from the generalized exponential distribution under Type-I censoring," *IEEE Transactions on Reliability*, 64, 31–43.

Hong, Y., King, C., Zhang, Y. and Meeker, W.Q. (2014), "Bayesian life test planning for the log-location-scale family of distributions," *Statistics Preprints*, 131, 1–25.

Kundu, D. and Ganguly, A. (2017), "*Analysis of step-stress models: existing results and some recent developments*," GB: Academic Press.

Lindley, D. V. (1956), "On a Measure of the Information Provided by an Experiment," *The Annals of Mathematical Statistics*, 27, 986–1005.

Mondal, S. and Kundu, D. (2020), "Bayesian inference for weibull distribution under the balanced joint Type-II progressive censoring scheme," *AMERICAN JOURNAL OF MATHEMATICAL AND MANAGEMENT SCIENCES*, 39, 56–74.

Nelson, W. (1980), "Accelerated life testing step-stress models and data analyses," *IEEE Transactions on Reliability*, 29, 103–108.

Samanta, D., Ganguly, A., Kundu, D. and Mitra, S. (2017), "Order restricted Bayesian inference for exponential simple step-stress model," *Communications in Statistics - Simulation and Computation*, 46, 1113–1135.

Turkkan, N. and Pham-Gia, T. (1997), "Highest posterior density credible region and minimum area confidence region: the bivariate case," *Journal of the Royal Statistical Society. Series C (Applied Statistics)*, 46, 131–140.

van Dorp, J.R., Mazzuchi, T.A., Fornell, G.E. and Pollock, L.R. (1996), "A Bayes approach to step-stress accelerated life testing," *IEEE Transactions on Reliability*, 45, 491–498.

Wu, S., Lin, Y. and Chen, Y. (2006), "Planning stepstress life test with progressively Type-I groupcensored exponential data," *Statistica Neerlandica*, 60, 46–56.

Xu, H. and Fei, H. (2012), "Models comparison for step-stress accelerated life testing," *Communications in Statistics - Theory and Methods*, 41, 3878–3887.